ISSN: 1410-8917
e-ISSN: 2597-9914

Jurnal Kimia Sains dan Aplikasi 26 (5) (2023): 166-177

Jurnal Kimia Sains dan Aplikasi
Journal of Scientific and Applied Chemistry

Journal homepage: http://ejournal.undip.ac.id/index.php/ksa

The potential of Myricitrin, a Flavonoid Compound in *Eugenia polyantha* from Indonesia, as an Antiviral Drug for SARS-CoV-2 through the Molecular Docking Analysis

Syamsul Falah [a,*], Laksmi Ambarsari [a], Dimas Andrianto [a], Rini Kurniasih [a], Sanro Tachibana [b]

[a] Department of Biochemistry, Faculty of Mathematics and Natural Sciences, IPB University, Kampus IPB Darmaga, Bogor, Jawa Barat, Indonesia
[b] Department of Applied Biosciences, Faculty of Agriculture, Ehime University, Ehime, Japan

* Corresponding author: syamsulfa@apps.ipb.ac.id

https://doi.org/10.14710/jksa.26.5.166-177

Article Info

Article history:

Received: 18th October 2022
Revised: 09th June 2023
Accepted: 22nd June 2023
Online: 31st July 2023

Keywords:
Eugenia polyantha; molecular docking; myricitrin; SARS- CoV- 2

Abstract

A Flavonoid glycoside compound, isolated and identified from *E. polyantha* as myricitrin, was analyzed as a ligand for its molecular binding activity against SARS-CoV-2 protein (receptor binding domain on Spike/RBD, main protease/nsp5, EndoRNAse, RNA-dependent-RNA-polymerase/RdRp), and its receptor, ACE2, and computationally assessed via molecular docking method. This study aims to determine the potential of myricitrin in *E. polyantha* from Indonesia as an antiviral drug for SARS-CoV-2 through molecular docking and molecular dynamic simulation analysis. The results showed that the myricitrin had the strongest binding affinity energy towards the three important SARS-CoV-2 proteins, namely endoRNAse, main protease (3CLpro), and RdRp with ΔG values of -9.60 kcal/mol, -8.40 kcal/mol, and -8.30 kcal/mol, respectively. These values are stronger than the comparator ligands of favipiravir (-5.60 kcal/mol), atazanavir (-7.20 kcal/mol), and remdesivir (-7.70 kcal/mol). This indicated that the compound has the potential as an inhibitor against 3CLpro, endoRNAse, and RdRp of SARS-CoV-2 proteins. This result was supported by the prediction made according to the Molprobity and PASS Online web servers, which showed that myricitrin has high bioactivity potential as an enzyme inhibitor (with a score of 0.38) and antiviral (with a score of 0.704).

1. Introduction

Severe acute respiratory syndrome coronavirus 2 (SARS-CoV-2) infection was first reported in 2019 and has since spread worldwide, causing more than 208,470,375 cases of COVID-19 and 4,377,979 deaths globally as of 18 August 2021 [1]. Indonesia confirmed its first positive case of COVID-19 on 2 March 2020 [2]. Within 40 days, cases of COVID-19 were reported by all provinces [3]. SARS-CoV-2 is a beta type in the coronavirus family enveloped with the single-stranded genetic material of RNA and has been identified to infect humans.

There are important target proteins in the search for its antiviral SARS-CoV-2 drug, and this includes spike, 3-chymotrypsin-like cysteine protease (3CLpro), or main protease (Mpro), papain-like protease (PLpro), RNA-dependent RNA polymerase (RdRp), and endoRNAse. The spike protein binds the virus to human receptors, a metallopeptidase called angiotensin-converting enzyme 2 (ACE2), while the 3CLpro and PLpro enzymes play a role in the packaging of new virions from viral polyproteins expressed on the ribosomes of the host cell, and RdRp replicates the SARS-CoV-2 genome [4]. Based on this, spike and nonstructural proteins (3CLpro, PLpro, RdRp, and endoRNAse) have been recognized as fundamental targets in computational strategies, such as molecular docking.

Presently, a special drug to stop the spread of SARS-CoV-2 is still in search and analysis. Therefore, drugs are

urgently needed to reduce the virus infection risk. Moreover, molecular docking is a powerful, rational, and low-cost approach that enables the analysis of ligand interactions on the active sites of target proteins and also supports the design and screening of active compounds, which are novel antiviral drugs against COVID-19.

Eugenia polyantha, known in Indonesia as bay leaf, has long been used as a spice in various types of cooking. Also, it is often used as traditional medicine for diseases, such as anti-ulcer, anti-diabetic, anti-inflammatory, and anti-diarrheal [5]. Various compounds have been isolated from *E. polyantha* with diverse biological activities, specifically hydroxycharvicol as a pancreatic lipase inhibitor [6]; rutin, catechin, and gallic acid as antioxidants [7].

In this study, a flavonoid glycoside was isolated from *E. polyantha* and identified as myricitrin. It was analyzed as a ligand for its molecular binding activity against SARS-CoV-2 proteins and its receptor, ACE2, and computationally assessed using molecular docking analysis. This study aims to determine the potential of myricitrin in E*. polyantha* from Indonesia as an antiviral drug for SARS-CoV-2 through molecular docking analysis. This analysis is recommended as a basis for developing natural compounds from *E. polyantha* as an antiviral drug for SARS-CoV-2 in future studies.

2. Methodology

A flavonoid glycoside compound was isolated and identified from *E. polyantha* as myricitrin with 2D Spectral Analysis (^{1}H- and ^{13}C-NMR) using NMR JEOL 500 MHz. It was elucidated by spectroscopic data and by comparison with the myricitrin NMR data from the reference. The myricitrin was analyzed as a ligand for its molecular binding activity against SARS-CoV-2 protein (receptor binding domain on Spike/RBD, main protease/nsp5, EndoRNAse, RNA-dependent-RNA-polymerase/RdRp); and its receptor, ACE2, and computationally assessed via molecular docking method and molecular dynamic simulation.

2.1. Plant Material

The *E. polyantha* leaves were collected from the tree planted at the University Farm of IPB. Then, the leaves were air-dried and ground to become powder. A voucher specimen was collected and deposited in the Tropical Biopharmaca Research Center, IPB University.

2.2. Extraction

The leaf powder (200 g) was successively extracted for 72 hours at room temperature with MeOH: water (9:1, v/v). In addition, another 200 g was extracted with MeOH: water (1:1, v/v). The 90% and 50% methanol-water extracts were mixed and then partitioned with n-hexane and chloroform to yield n-hexane, chloroform, and aqueous fractions. The aqueous fraction was used for further analysis.

2.3. Isolation and Identification of Compounds

The aqueous fraction (7.7 g) was chromatographed on a silica gel column (EtOAc: acetone: acetic acid: H_2O (v/v) as step gradient solvent). Then, 120 fractions were collected and pooled to become six (frs. 1~6). Fr. 1 was then separated by Thin Layer Chromatography (TLC) (RP-18, F254 S, Merck) with EtOAc: acetone: acetic acid: H_2O (60:20:10:10, v/v) as elution solvent to produce eight fractions (frs. 1-1~1-8). Fr. 1-5 were repurified by preparative TLC with MeOH: H_2O (3:2, v/v) as elution solvent to yield five fractions (frs. 1-5-1~1-5-5). Fr. 1-5-4 were then purified using HPLC to produce a pure compound, which was identified and analyzed with 2D Spectral Analysis (^{1}H- and ^{13}C-NMR) using NMR JEOL 500 MHz.

2.4. Target Protein Characterization

Molecular docking was performed using Autodock Vina software. Initially, several analyses were carried out regarding the characteristics of the target protein, including 1) a literature review of their active site, 2) a homology analysis of the target protein sequences against the Protein Data Bank (PDB) using a BLAST server, and 3) alignment of these sequences with those that have high homology, based on the results of previous analysis, performed using Clustal Omega.

2.5. Preparation of Ligand Structures and Target Proteins

The determination of the ligand structure and target protein were carried out using the methods of Krieger and Vriend [8] with modifications. The 3D structure of myricitrin, an active compound that has been isolated and identified from *E. polyantha* as a test ligand, with several other ligands was used as a comparison, including the flavonoid myricetin, favipiravir, remdesivir, and hydroxychloroquine because they have potential as an antiviral drug against SARS-CoV-2. The 3D structure of the test and comparison ligands were downloaded in .sdf format from the database of chemical compounds, PubChem (https://pubchem.ncbi.nlm.nih.gov/). The ligand structure obtained was then optimized by adding hydrogen to the right atom using Discovery Studio, then optimizing the geometry through the energy minimization method using the YASARA model by running the macro em_runclean.mcr file (water solvent in a 1A simulation box) to form the optimum conformation at minimum global energy. The optimized 3D ligand structure was saved in .pdb file format for the molecular docking process.

The target protein structures were downloaded from the Protein Data Bank (http://www.rcsb.org/), including the Receptor binding domain structure on the spike protein (RBD) and Angiotensin-converting Enzyme (ACE2) from the RBD spike-ACE2 complex (PDB) ID 6VSB: A), Main protease (PDB ID 6lu7), and EndoRNAse (PDB ID 6w01). While the RNA-dependent-RNA-polymerase (RdRp) structure was obtained based on the homology modeling method, using the SWISS Model server with the RdRp sequence SARS-CoV-2 (YP_009725307.1) as the template [9]. Furthermore, the SARS-CoV-2 RdRp structure from the modeling results was minimized to obtain the best and most stable structural conformation using the YASARA server by running the em _runclean.mcr program. Each target

protein structure was prepared using Autodock tools software. Furthermore, these proteins were stored as receptors in the .pdbqt file format.

2.6. Validation of Molecular Docking Parameters

The grid size was validated by redocking the co-crystal ligand molecules of each target protein to their active site. Several target proteins of SARS-CoV-2 that have co-crystal ligands are the main protease (PDB ID 6LU7) and endoribonuclease/NSP15 (PDB ID 6W01). The molecular docking of co-crystal ligands was carried out 20 times for each grid box size analyzed, with the lowest RMSD value as the optimum grid box size. The RMSD values were calculated using the Discovery studio by combining (superposing) the same two molecules, specifically, the co-crystal ligand resulting from redocking with those attached to each receptor. Meanwhile, validation for other target proteins that did not have a co-crystal ligand was through the targeted molecular docking of a comparison ligand at its active site. These target proteins included the spike protein (RBD) and Angiotensin-converting Enzyme (ACE2) from the RBD spike-ACE2 complex (PDB) ID 6VSB: A), and the RNA-dependent-RNA-polymerase (RdRp) structure was obtained based on the homology modeling method. The best grid box volume was selected based on its free energy of binding (ΔG_{bind}) value and its docking on the active site.

2.7. Ligand Molecule Docking Towards the Target Protein

The ligand molecular docking was analyzed towards proteins using the optimum grid box size obtained from the validation of each target protein. In the autodock tools software, the target protein file was inputted in the .pdbqt format obtained from the previous preparation. Subsequently, the ligand structure in .pdb format was inputted into the autodock tools via their menu. Previously, the parameterization of the ligand was carried out by adjusting their torsion to become rotatable and saved in the file format ligand.pdbqt. Another parameter was the determination of the grid box size for the target protein using the validation results and saved in the gridbox.txt file format.

Molecular docking analysis was executed with the Vina program via the command vina.exe –config config.txt –log log.txt –out.pdbqt. Furthermore, the results obtained included the value of ΔG_{bind}, the dissociation constant value of each ligand against the target protein using the YASARA automatic molecular docking structure, and the intermolecular interactions of the ligands against the target protein were analyzed using the LigPlot+ program.

2.8. Analysis of Pharmacokinetic Properties, Bioavailability, and Bioactivity

The pharmacokinetic properties to predict drug-likeness was analyzed with Lipinski's rule of five (RO5) parameters (http://www.scfbio- iitd.res.in/software/drugdesign/lipinski.jsp) [10]. ADME properties and bioavailability were analyzed with the Swiss ADME web server (http://www.swissadme.ch/) [11]. Drug bioactivity can be determined by estimating the activity scores of GPCR ligands, ion channel modulators, nuclear receptor ligands, kinase inhibitors, protease inhibitors, and enzyme inhibitors. All parameters were determined with the Molinspiration drug-likeness score online (www.molinspiration.com), which was performed by selecting the "Calculation of Molecular Properties and Prediction of Bioactivity" menu [12]. To support the prediction of the potential of myricitrin as a candidate antiviral compound, the PASS Online web server was used to predict biological activity, including pharmacological effects, mechanisms of action, toxic and adverse effects, interactions with metabolic enzymes and transporters, influences on gene expression, including antiviral activity and others.

2.9. Molecular Dynamic Simulation

Based on the results of myricitrin docking on SARS-CoV-2 proteins, the strongest affinity of myricitrin was shown in endoRNAse. The myricitrin-endoRNAse complex was then analyzed for the stability of its interaction through molecular dynamic simulation. The result of docking myricitrin to endoRNAse was used as the initial conformation of the molecular dynamic simulation. MD simulation of the myricitrin-endoRNAse complex was performed using the YASARA Structure software. This procedure was carried out using the AMBER14 force field. The cell extension on each side around the solute measures 10 Å from the cube box wall with periodic boundary conditions. The TIP3P water model was selected for solvating complexes, followed by adding ions to neutralize. MD simulation was done using NVT and NPT ensemble for 30000 ps or 30 ns [13]. The trajectories were set to be generated save every 250 ps. The energy was minimized using the steepest descent method. Berendsen temperature coupling and isotropic pressure coupling were established in order to reach a stable environment (300 K, 1 bar). The protein-ligand complexes results were then analyzed. The stability of the myricitrin-EndoRNAse complex interaction was seen based on the RMSD and RMSF [13].

3. Results and Discussion

3.1. Isolation and Identification of Compounds

The purification and isolation results of the methanol extract of *E. polyantha*, followed by identification using NMR, showed a myricitrin compound A. Based on the spectroscopic data in Table 1, there were three aromatic signals in the ^{1}H-NMR spectrum, namely two doublets at δ 6.20 (1H, J = 2.1 Hz, H-6) and δ 6.30 (1H, J = 2.1 Hz, H-8), and one broad singlet (2H, H-2 'and -6') in addition to ^{13}C-NMR peaks at δ 99.8, 94.7, and 109.6. In addition, ^{1}H- and ^{13}C-NMR data showed a chemical shift for sugar moiety at δ 5.31 (1H, s), 4.22 (1H, d, J = 1.8 Hz), 3.77 ~ 3.81 (1H, m), 3.34 (1H, m), 3.50 ~ 3.53 (1H, m), 0.96 (3H, d, J = 6.3 Hz), and 17 carbon signals indicating the presence of myricetin structure, and O-glycosidic linkage bonds on rhamnoside moiety at position C-3 (δ 136.4). The NMR was identical to the reference data from previous studies [14]. Based on the reference, the compound was identified as myricetin-O-rhamnoside, also known as myricitrin (Figure 1).

Table 1. ^{1}H- and ^{13}C-NMR data of myricitrin (CD_3OD, 500 MHz)

Position	δ_H (mult) (*J* in Hz)	δ_C	Reference [14]	
			δ_H (mult) (*J* in Hz)	δ_C
2		159.5		159.2
3		136.4		136.1
4		179.7		179.5
5		163.3		163.1
6	6.20 *d* (2.1)	99.8	6.19 *d* (1.8)	99.7
7		165.9		164.0
8	6.36 *d* (2.1)	94.7	6.35 *d* (2.3)	94.6
9		158.5		158.4
10		105.9		105.6
1’		121.9		121.7
2’	6.95 br,*s*	109.6	6.94 *s*	109.6
3’		146.9		146.7
4’		137.9		137.7
5’		146.9		146.7
6’	6.95 br,*s*	109.6	6.94 *s*	109.6
1”	5.31 *s*	103.7	5.30 *d* (1.8)	103.5
2”	4.22 d (1.8)	71.9	4.21 *dd* (3.2, 1.8)	71.7
3”	3.77~3.81 *m*	72.1	3.76~3.78 *dd* (9.4, 3.4)	72.0
4”	3.34 *m*	73.4	3.31~3.34 *m*	73.2
5”	3.50~3.53 *m*	72.1	3.48~3.54 *m*	71.9
6”	0.96 *d* (6.3)	17.7	0.94~0.96 *m*	17.5

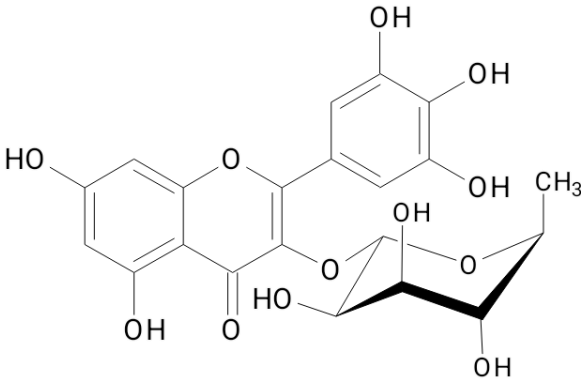

Figure 1. Myricitrin structure from *E. polyantha*

3.2. Validation of Molecular Docking Parameters

Docking validation is an important initial step to assess docking quality. For target proteins complexed with a ligand (co-crystal ligand), docking validation was done by redocking the co-crystal ligand to the protein. The best grid box volume was determined based on the RMSD value between the redocked co-crystal ligand and the co-crystal ligand. The smaller the RMSD value, the more similar the conformation of the redocked co-crystal ligand to the initial co-crystal ligand at a certain grid box size. In this study, two target proteins have co-crystal ligands: main protease (PDB ID 6LU7) and endoribonuclease/NSP15 (PDB ID 6W01). The main protease (PDB ID 6LU7) has a co-crystal ligand that acts as an inhibitor of the main protease, namely N3 [15]. Endoribonuclease/NSP15 (PDB ID 6W01) has citrate as a co-crystal ligand docked to the active site [16].

Based on the results of docking validation on the main protease (PDB ID 6LU7), the best grid box volume was grid box with coordinates of -7.752, 13.523, and 68.459 (coordinate center x, y, and z) and size of 30, 32, 30 (size x, y, z). Redocking the co-crystal ligand N3 to the main protease with the grid box produced a conformation very similar to the co-crystal ligand N3 with a low RMSD value of 0.0480 Å (Figure 2A). In the 3D structure of endoRNAse (PDB ID 6W01) there is citrate as a co-crystalline ligand. Citrate acts as a stabilizer for this enzyme which is anchored to the active site. Based on the results of docking validation on endoribonuclease/NSP15 (PDB ID 6W01), the best grid box volume was grid box with coordinates -65.869, 71.929, and 28.813 (coordinate center x, y, and z), and size of 32, 32, and 42 (size x, y, and z). Redocking of citrate to endoRNAse with the best grid box resulted in a conformation that was quite similar to citrate with an RMSD value of 1.800 Å.

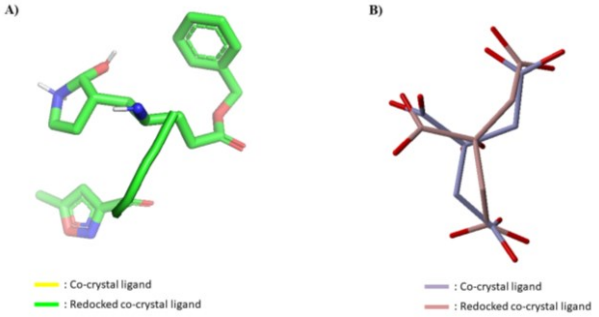

Figure 2. Superpose the redocked co-crystal ligand with the co-crystal ligand in docking validation. A) Superpose the redocked N3 with the co-crystal N3 in the main protease, B) Superpose the redocked citrate with the co-crystal citrate in endoRNAse

3.3. Receptor Binding Domain (RBD) of SARS-CoV-2 Spike

Based on the results of the homology analysis, the SARS-CoV-2 spike protein sequence has a 76% similarity to the SARS-Cov spike (Table 2). In the multi-sequence alignment in Figure 2, there are differences in the amino acids forming the SARS-CoV-2 spike with SARS-CoV. This was mainly in the amino acids forming the receptor-binding motif (RBM). These differences play an important role in determining the nature of the virus, strengthening the binding of the SARS-CoV-2 spike to ACE2. In the SARS-CoV-2 genome, mutations were quite high compared to the SARS-CoV genome. One of these mutations occurred in the spike protein sequence. The amino acids that compose RBD and RBM of SARS-CoV-2 largely differed from RBD and RBM of SARS-CoV [17]. This difference played an important role in determining the infection mechanism of SARS-CoV-2 [18, 19].

Spike is the outermost structural protein in SARS-CoV-2 which plays an important role in the early stages of viral infection in its host cells. The binding of spike proteins to ACE2 via RBD has a strong affinity, facilitating the entry of SARS-CoV-2 genetic material into the human

body. In the SARS-CoV-2 spike RBD, the receptor binding motif (RBM) composed of amino acids 437-508 interacts with the amino acid ACE2 [20]. The five essential amino acids in the RBM Spike SARS-CoV-2 bind to the ACE-2 receptor are Leu455, Phe486, Gln493, Ser494, and Asn501 (Figure 3).

Myricitrin is 3-O-α-L-rhamnopyranoside of myricetin. Myricetin was used as a comparison ligand in this study because it is a flavonoid compound with structural similarities to myricitrin. Another comparison ligand is hesperidin. Based on Ahmad *et al.* [21], hesperidin disrupts the interaction between ACE2 and RBD. The affinity of the ligand to the target protein is determined based on the value of ΔG_{bind}, inhibition constant (Ki), and molecular interactions with RBD of SARS-CoV-2. The more negative of ΔG_{bind} value, the smaller the Ki. This showed a stronger binding affinity between the ligands to the target protein.

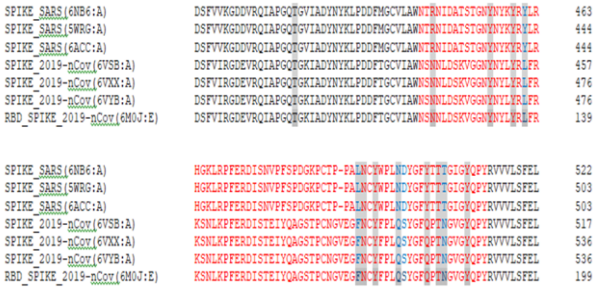

Figure 3. Comparison of the SARS-CoV-2 and SARS-Cov spike sequences. The red was a region-binding motif (RBM) sequence in the region-binding domain (RBD) of Spike SARS-CoV-2. The gray shadow sequence was an amino acid interacting with ACE2. The blue sequences were the five essential amino acids Spike SARS-CoV-2 in binding to the ACE-2 receptor

Based on molecular docking results, all ligands were docked to the SARS-CoV-2 spike, especially in the RBD pocket (Figure 4A). Myricitrin showed a stronger binding affinity for the RBD of the SARS-CoV-2 spike than myricetin, indicated by a ΔG_{bind} value of -6.9 kcal/mol and a Ki of 8.642 µM (Table 3). On the other hand, myricitrin showed slightly lower binding affinity than hesperidin (Table 3). Another important aspect was analyzing the interaction between ligand molecules and the target protein using the Ligplot. It showed the interaction of myricitrin with several important amino acids on the RBM of the SARS-CoV-2 spike (Figure 4B). These include hydrogen bonds between myricitrin and Ser494 and hydrophobic interactions with several important amino acids in RBM, namely Leu455 and Tyr505 [21]. Moreover, Leu455 and Ser494 played an important role in binding SARS-CoV-2 to ACE2 receptors. This showed that the myricitrin compound from the *E. polyantha* extract has an inhibitor potential toward SARS-CoV-2 spike interaction with ACE2 in the early stages of infection.

Table 2. Homology of SARS-CoV-2 and SARS-CoV protein sequences

Protein SARS-CoV-2	SARS-CoV-2 (%)	SARS-CoV (%)
Spike	99.50	76
RdRp (nsp12)	100	96.35
Main Protease	100	96 (3C-Like Proteinase)
Endonuclease (nsp15)	100	88.73

Table 3. Free energy of ligand binding to the SARS-CoV-2 target protein

Target Protein	Compound	Type of Ligand	ΔG_{bind} (kcal/mol)	Ki (µM)
RBD	Myricitrin	Test	-6.900	8.642
	Myricetin	Reference	-5.800	55.443
	Hesperidin	Reference	-7.700	2.237
Main Protease	Myricitrin	Test	-8.300	0.812
	Myricetin	Reference	-7.300	4.397
	Atazanavir	Reference	-7.200	5.206
RdRp	Myricitrin	Test	-8.300	0.812
	Myricetin	Reference	-7.500	3.136
	Remdesivir	Reference	-7.700	2.237
Endo-RNAse	Myricitrin	Test	-9.600	0.090
	Myricetin	Reference	-8.400	0.685
	Favipiravir	Reference	-5.600	77.735
ACE2	Myricitrin	Test	-6.300	23.820
	Myricetin	Reference	-6.100	33.397
	Paritaprevir	Reference	-6.700	12.117

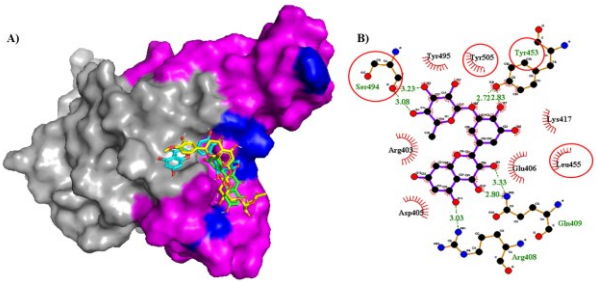

Figure 4. Interaction of myricitrin compounds against RBD Spike SARS-CoV-2. A) Myricitrin and reference ligands docked to RBD Spike SARS-CoV-2; RBD Spike SARS-CoV-2 was presented in a surface structure: magenta (RBM), and blue (the five essential amino acids of RBM Spike SARS-CoV-2 in binding to the ACE-2 receptor); Ligands were presented in stick structure: cyan (myricitrin), green (myricetin), yellow (hesperidin). B) Myricitrin intermolecular interactions with RBD Spike SARS-CoV-2: Purple (myricitrin) and brown stick molecules (amino acid RBD of SARS-CoV-2 spike hydrogen-bond with ligands). The green dotted lines and the numbers showed the length of hydrogen bonds, the arc indicated hydrophobic interactions of amino acids, while the red circles are RBM of the SARS-CoV-2 spike

3.4. Main Protease (nsp5) of SARS-CoV-2

The SARS-CoV-2 main protease known as 3CL-protease is a proteolytic enzyme encoded by the nonstructural protein 5 (nsp 5) gene in the ORF1a SARS-CoV-2 region, one of the drug targets for the antiviral assessment of SARS-CoV-2. Its structure used in this analysis is the SARS-CoV-2 main protease with the code PBD ID 6lu7. In this study, two comparison ligands were used, namely myricetin and atazanavir. According to Xiao *et al.* [22], myricetin can potentially be a candidate drug for COVID-19 therapy as an anti-SARS-CoV-2 through inhibition of main proteases and anti-inflammation. Atazanavir is an anti-retroviral FDA-approved medication commonly used for HIV treatment and prevention by inhibiting protease activity [23]. According to Fintelman-Rodrigues *et al.* [24], atazanavir can bind strongly to the active site of the main protease of SARS-CoV-2 because it has strong bioavailability in the respiratory tract so that atazanavir can inhibit the replication of SARS-CoV-2. This is also supported by the research of Chaves *et al.* [25], which stated that atazanavir is a competitive inhibitor of SARS-CoV-2 Mpro, interfering with the replication of SARS-CoV-2 genetic material by in vitro and in vivo. Based on this, myricetin and atazanavir are ideally used as comparator ligands in determining the potential of myricitrin as a main protease inhibitor.

Based on molecular docking results, myricitrin showed the strongest binding affinity for the main protease SARS-CoV-2 based on the value of free binding energy (ΔG) and the Ki (Table 3). Myricitrin compound from *E. polyantha* showed the strongest binding affinity with the most negative free energy (ΔG) value of -8.3 kcal/mol and the smallest Ki of 0.812 µM. Myricitrin has a more negative ΔG value than myricetin and atazanavir. This was supported by the intermolecular interactions that showed these compounds reacting with several important catalytic amino acids in the SARS-CoV-2 main protease (Figure 5).

The main protease SARS-CoV-2 used in this analysis was a polypeptide monomer composed of three domains (Figure 5), including I (amino acid residues 1-101) and II (residues 102-184). The domain plays a role in the formation of a double-barrel that is similar to the structure of the main protease of SARS-CoV [26], and domain III C-terminal-helical (residue 201-301) plays a role in the formation of dimeric structures (dimerization of polypeptides) and were required for catalytic activity. This was because the main protease decreased its catalytic activity when the C-terminal-helical III domain was removed [27]. The active site for the main protease was located between domains I and II, which consisted of several amino acids.

The myricitrin interacts with a large number of catalytic amino acids' main proteases, which was shown in Figure 5, including hydrogen bonds with the residues of Leu141, Ser144, Cys145, and His163, as well as hydrophobic interactions with His41, Phe140, Asn142, and Gly143. The amino acid residues were part of the catalyst that played a role in the binding of the substrate and the catalytic activity of the main protease enzymes, such as dyad Cys145-His41. Based on the results, myricitrin has the potential as an inhibitor of the SARS-CoV-2 main protease enzyme.

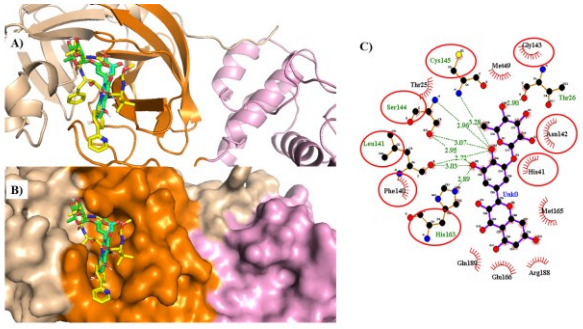

Figure 5. The interaction of myricitrin from E. polyantha on the SARS-CoV-2 main protease. A) Myricitrin and reference ligands docked to the main protease in a cartoon view. B) Myricitrin and reference ligands docked to the main protease in a surface view. In the structure, there are myricitrin (cyan), myricetin (green), and atazanavir (yellow). This included light brown surface (domain I), orange surface (domain II), and pink surface (domain III C terminal-helical). C) Myricitrin intermolecular interactions with the main SARS-CoV-2 protease. This included purple (myricitrin) and brown stick molecule (amino acid main protease SARS-CoV-2, which bonds hydrogen with ligands), green dotted line (hydrogen bond), green numbers (hydrogen bond length), red circle (acid catalytic amino at the active site), and red lashes (hydrophobic interaction of amino acids against ligands)

3.5. RNA-dependent RNA Polymerase (RdRp) nsp12 of SARS-CoV-2

RNA-dependent RNA polymerase (RdRp) is an important enzyme that catalyzes the replication and transcription of SARS-CoV-2 ssRNA in its host [28]. The SARS-CoV-2 RdRp protein sequence has high homology to the SARS-Cov RdRp of 96.35–100%. Based on research by Gao *et al.* [28], the active site of the SARS-CoV-2 RNA-dependent RNA polymerase protein is in seven conserved motifs from A to G (Figure 6A). Residues ASP618, SER759, ASP760, and ASP761 are RdRp protein catalytic sites located in motifs A and C. The active site plays an important role in the ligand-binding region. The active site consists of two functional regions, which recognize the substrate (substrate binding site) and catalyze chemical reactions (catalytic site) [29].

Myricitrin and two comparison ligands (myricetin and remdesivir) have a strong binding affinity for the SARS-CoV-2 RdRp protein. This was indicated by the value of the most negative of free binding energy (ΔG) (Table 3), which was -8.4 kcal/mol (myricitrin), -7.5 kcal/mol (myricetin), and -7.5 kcal/mol (remdesivir), respectively. The strength of the binding affinity was also supported by the low Ki, 0.812 µM for myricitrin, 3.136 µM for myricetin, and 2.237 µM remdesivir, respectively. In this study, myricetin as a comparison ligand is not only a flavonoid compound similar to myricitrin but also because this compound has certain therapeutic effects on COVID-19 [30]. Based on the study of Olender *et al.* [31], COVID-19 patients treated with remdesivir showed

significantly greater recovery and 62% reduced odds of death versus standard-of-care treatment in patients with severe COVID-19, particularly through inhibition of the SARS-CoV-2 RdRp protein [32]. Therefore, in this study, remdesivir was also used as a comparison ligand to determine the potency of myricitrin as a SARS-CoV-2 RdRp protein inhibitor.

Myricitrin was the strongest affinity for SARS-CoV-2 RdRp protein, with the lowest ΔG_{bind} value of -8.4 kcal/mol (Table 3). Furthermore, the intermolecular interactions of the ligands on the target protein also showed the degree of binding affinity of a ligand, as shown in Figure 6. The myricitrin compounds have more hydrogen bonding interactions than remdesivir and myricetin, including hydrogen bonds with the catalytic amino acid Ser759 and several amino acids as the binding sites of RdRp inhibitors, such as Arg555 [28]. The amino acid Arg555 played a role in facilitating the entry of NTP at the catalytic site for the polymerization of SARS-CoV-2 RNA [28]. The hydrogen bond formed between the myricitrin and Arg555 was predicted to inhibit the polymerization activity of SARS-CoV-2 RNA by RdRp.

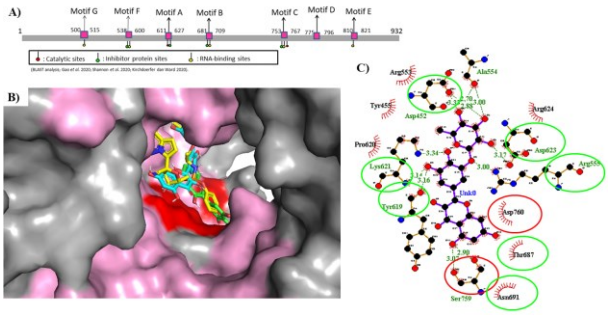

Figure 6. Interaction of myricitrin compounds *E. polyanta* from Indonesia against RdRp SARS-CoV-2. A) Map of SARS-CoV-2 RNA-dependent RNA polymerase sequences with motifs and catalytic sites, B) Myricitrin and reference ligands docked to RdRp in a surface view. In the structure, there are myricitrin (cyan), myricetin (green), and remdesivir (yellow), pink color is the active site, and red color is catalytic sites (catalytic amino acids: ^{618}D-xxx-$^{759}SDD^{761}$), C) The intermolecular interactions of the myricitrin to the RdRp of SARS-CoV-2 spike, consisted of myricitrin (purple stick). The green dotted line and numbers are hydrogen bonds and the length. The eyelashes are hydrophobic interactions of amino acids and ligands. The green circles are active site amino acids, and the red circles are catalytic amino acids.

3.6. SARS-CoV-2 EndoRNAse

EndoRNAse is one of the ideal targets for the design of SARS-CoV-2 antiviral therapy. The 3D endoRNAse structure used in this analysis was endoRNAse with code PDB 6W01. In the endoRNAse (6W01) structure, two loops played an important role in substrate interaction, specifically the supporting and the active site loop. In both, active site amino acids play a role in the catalytic activity of endoRNAse enzymes, such as His259, His264, Lys314, Ser318, Thr365, and Tyr367 (Figure 7).

Based on the molecular docking results in Table 3, the myricitrin compound *E. polyantha* showed the strongest binding affinity among other ligands with the most negative ΔG_{bind} value of -9.6 kcal/mol and the lowest Ki of 0.090 µM. The myricetin is a comparison ligand from the flavonoid group showing a second strong binding affinity after the flavonoid compound from *E. polyantha* with a ΔG_{bind} value of -8.4 kcal/mol and Ki of 2.237 µM. The strong binding affinity of the two flavonoid compounds strengthens the prediction that these compounds have a strong potential as an inhibitor of the endoRNAse enzyme SARS-CoV-2 (6W01).

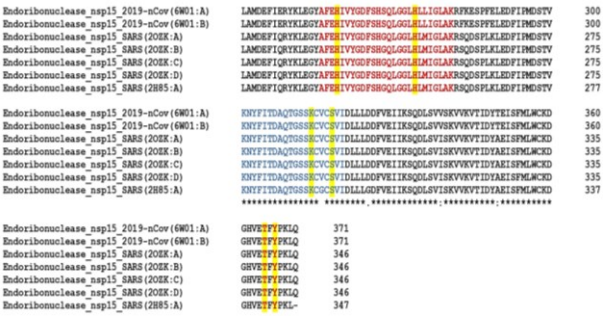

Figure 7. Important regions of the SARS-CoV-2 endoRNAse enzyme. The red, blue, and yellow amino acids are the active and supporting loops, and the catalytic amino acids, respectively

According to Manabe *et al.* [33], favipiravir showed a high potential for treating Covid-19 patients. Based on Manabe's research, early use of favipiravir in COVID-19 patients can increase viral clearance within 7 days and clinical improvement within 14 days, especially for mild symptoms. In this study, favipiravir was used as one of the comparison ligands. Myricitrin had the most negative ΔG_{bind} value compared to favipiravir and myricetin (Table 3). Based on the most negative ΔG_{bind} value, myricitrin has the potential as a drug candidate for treating COVID-19 through inhibition of the SARS-CoV-2 endoRNAse.

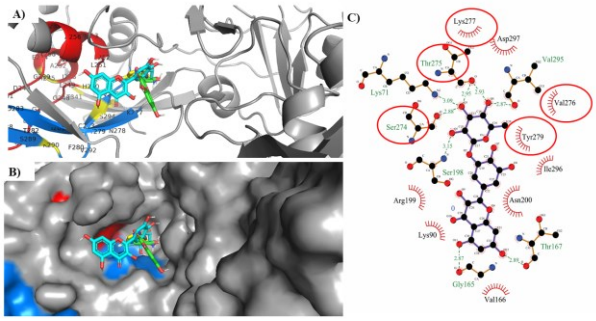

Figure 8. Interaction of the myricitrin compound *E. polyantha* from Indonesia against endoRNAse SARS-CoV-2. A) Myricitrin and reference ligands docked to endoRNAse in a cartoon structure. B) Myricitrin and reference ligands docked to endoRNAse in the surface structure. Gray (endoRNAse polypeptide chain), red (active site loop), blue (supporting loop), yellow (catalytic amino acid). In the structure, there are myricitrin (cyan), myricetin (green), and favipiravir (yellow). C) Intermolecular interactions of myricitrin to endoRNAse SARS-CoV-2 included the purple (myricitrin) and brown stick molecule (amino acid endoRNAse SARS-CoV-2 hydrogen bonds with ligands). The green dotted line and numbers (hydrogen bond and length). Red circle and arc (amino acid loop active site and their hydrophobic interaction with ligands)

Another parameter that supports the potential of myricitrin as a COVID-19 drug candidate by inhibiting

endoRNAse is its intermolecular interactions. The intermolecular interactions showed that myricitrin reacted with several amino acids in the active site loop, including hydrogen bonds with amino acids Ser274 and Thr275 and hydrophobic interactions with Val276, Lys277, and Tyr279. The overall interactions between myricitrin and the SARS-CoV-2 endoRNAse were five hydrogen bonds and nine hydrophobic interactions, as shown in Figure 8. These interactions illustrated that the strong binding affinity aligned with the free energy of binding obtained.

3.7. Angiotensin Converting Enzyme 2 (ACE2) Protein Receptor

ACE2 is expressed in a large number of tissues and organs. The highest expression of ACE2 was in the alveolar epithelial cells of the lungs, small intestine enterocytes, arterial, venous, and smooth muscle cells in many organs. In addition, ACE2 was highly expressed in renal, cardiovascular, and gastrointestinal tissues [33, 34]. Also, it was the main target receptor for SARS-CoV-2 as a transmission route for viruses into human cells.

Because the ACE2 protein played an important role in the SARS-CoV-2 infection process, inhibiting the interaction of SARS-CoV-2 with ACE2 was very potential in treating COVID-19. ACE2 protein has also become a target in the search for SARS-CoV-2 therapy based on the mechanism of inhibiting RBD-ACE2 interactions. Therefore, ACE2 became one of the targets analyzed through molecular docking with myricitrin to inhibit SARS-CoV-2 RBD infection in this study. Based on the molecular docking test results, the lowest ΔG_{bind} value of -6.7 kcal/mol was paritaprevir as a comparative ligand, which was -6.7 kcal/mol with a low Ki of 12.117 µM (Table 3). Myricitrin (test ligand) and myricetin (comparative ligand) from the flavonoid group showed similar ΔG_{bind} values of -6.3 kcal/mol and -6.1 kcal/mol, respectively. Myricitrin's ΔG_{bind} value was slightly higher than paritaprevir, which was -6.3 kcal/mol with a low Ki of 23.820 µM. The smaller the dissociation constant, the more difficult it was for the ligand to escape from the receptor. Paritaprevir is used for the treatment of hepatitis C virus and parasitic infections. Based on the research of Ahmad *et al.* [21], paritaprevir has the strongest binding affinity for the ACE2 receptor in silico and can be used as a drug candidate for the treatment of COVID-19 by inhibiting the interaction of SPIKE SARS-CoV-2 with its receptor, ACE2. Based on the ΔG_{bind} values and Ki, this indicated that myricitrin from *E. polyantha* (Indonesia) can block the interaction between RBD SARS-CoV-2 and ACE2 by binding to ACE2 [35].

Based on the intermolecular interactions, myricitrin showed interactions with several important amino acids that played a role in the binding of RBD of SARS-CoV-2 spike in the transmission material genetic, as shown in Figure 9. Two hydrogen bonds were formed between myricitrin and the amino acids ACE2, namely Lys32 and Glu35. Both were important sustainable amino acid binding sites for the RBD of the SARS-CoV-2 spike. This showed that the myricitrin compound *E. polyantha* has the potential as a drug for COVID-19 by inhibiting the interaction between RBD of SARS-CoV-2 and its receptor, ACE2.

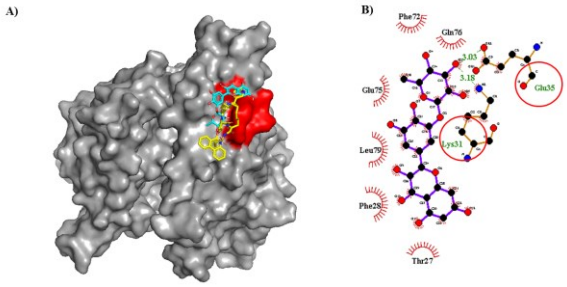

Figure 9. Interaction of myricitrin compounds from *E. polyantha* against human ACE2. A) Myricitrin and reference ligands docked to ACE2 in a surface structure consisting of ACE2 polypeptide chain (grey), the amino acid binding site of RBD of SARS-CoV-2 spike (red), myricitrin (the cyan stick), peritaprevir (the yellow stick). C) Myricitrin intermolecular interactions with ACE2, comprised of purple (myricitrin) and brown stick molecule (a sustainable amino acid ACE2 that bonds hydrogen with ligands). The green dotted line and their numbers (hydrogen bond and length). Red circle and Arc (sustainable amino acid binding site for RBD of SARS-CoV-2 spike and their hydrophobic interaction with ligands)

3.8. Pharmacokinetic Properties of Myricitrin Compound from *E. polyantha*

Analysis properties of pharmacokinetics, such as the suitability of Lipinski's rule of five, ADMET (Absorption, Distribution, Metabolism, Excretion, Toxicity), and bioactivity, were important parameters in assessing the potential of drug active compounds (Table 4). Based on this analysis, myricitrin has pharmacokinetic properties that meet the three properties of Lipinski's rule of five. Another characteristic, namely ADMET, was related to the process a drug compound passes through when administered orally. Based on the ADMET properties obtained, the myricitrin had a fairly good solubility with strong lipophilicity (Log P <5). This lipophilicity affected drug absorption, bioavailability, and toxicity. Log P value <5 indicated that the molecule has good hydrophobicity related to good membrane permeability properties, making it suitable for drug design. However, based on TPSA parameters, the percentage (%) and gastrointestinal absorption (GI) showed that these compounds were inappropriate for oral drug administration. This was reinforced by the prediction of its toxicity, indicating acute oral type III toxicity, meaning that the compound was toxic when ingested with an LD_{50} value between 50–300 mg/kg. However, myricitrin was unpredicted to be carcinogenic. Therefore, this prediction is developed in further research in vitro to in vivo to determine the nature of the toxicity, effectiveness, and the appropriate drug administration in inhibiting several types of SARS-CoV-2 and ACE2 target proteins for the treatment of COVID-19.

Table 4. Pharmacokinetic properties, ADMET, and ligand bioactivity

Parameter	Myricitrin	Myricetin	Favipiravir	Remdesivir	Hesperidin	Atazanavir	Paritaprevir
Molecular Weight (g/mol)	464.38	358	157	602	610	704	765
Hydrogen bond donor	8	6	1	3	8	5	3
Hydrogen bond acceptors	12	8	5	13	15	13	14
LogP	0.217	1.716	-0.549	0.500	-1.156	3.227	5.659
Molar Refractivity	106.526	75.715	32.187	133.614	140.698	188.197	208.137
Lipinski (drug-likeness)	Yes (2 violations)	Yes (1 violation)	Yes (1 violation)	No (3 violations)	No (3 violations)	No (3 violations)	No (3 violations)
ADMET:							
TPSA (Å²)	210.51	151.59	88.84	213.36	234.29	171.22	198.03
%Absorption	36.374	56.70	78.35	35.39	47.77	56.13	96.95
Water solubility	Soluble	Soluble	Very soluble	Moderately soluble	Moderately soluble	Poorly soluble	Poorly soluble
GI absorption	Low	Low	High	Low	Low	Low	Low
Log Kp (skin permeation) (cm/s)	-8.77	-7.40	-7.66	-8.62	-10.12	-6.62	-7.67
Bioavailability score	0.85	0.55	0.55	0.17	0.17	0.17	0.17
Carcinogens	Non-carcinogen	Non-carcinogen	Non-carcinogen	Non-carcinogen	Non-carcinogen	Non-carcinogen	Non-carcinogen
Acute oral toxicity	III	II	III	III	III	III	III
Bioactivity score by Molinspiration web server:							
GPCR ligand	-0.02	-0.06	-0.62	0.27	-0.01	-0.41	-0.78
Ion channel modulator	-0.08	-0.18	-0.44	-0.35	-0.59	-1.66	-2.24
Kinase inhibitor	0.08	0.28	-0.31	0.20	-0.36	-1.17	-1.79
Nuclear receptor ligand	0.14	0.32	-1.50	-0.48	-0.20	-1.39	-2.15
Protease inhibitor	-0.06	-0.20	-0.91	0.49	-0.00	0.26	-0.12
Enzyme inhibitor	0.38	0.30	-0.33	0.38	0.06	-0.70	-1.24
Bioactivity score by Molinspiration web server:							
Activity	Antiviral (Influenza)	Antiviral (Hepatitis B)	Antiviral (Influenza)	Antiviral	Antiviral (Herpes)	Antiviral	Antiviral (Hepatitis)
Probability active score (Pa)	0.704	0.519	0.662	0.814	0.550	0.679	0.874
Probability inactive score (Pi)	0.005	0.004	0.008	0.004	0.006	0.004	0.001

The docking molecular results showed that myricitrin had the strongest binding affinity for three important SARS-CoV-2 enzymes: main protease (3CLpro), endoRNAse, and RdRp (Table 3). This was supported by the bioactivity prediction according to the Molinspiration web server, which showed that the myricitrin compound has high bioactivity as an enzyme inhibitor with a value of 0.38. Based on Kulkarni *et al.* [36], for organic molecules, the probability is that if the bioactivity score is more than 0, it means active; values -5.0 to 0.0 means moderately active, and if less than -5.0, then inactive. This study showed that myricitrin was predicted to be active as an enzyme inhibitor based on the bioactivity score.

The prediction of the potential of myricitrin as a candidate for a SARS-CoV-2 antiviral drug was also strengthened by bioactivity predictions through the PASS

Online web server. The PASS Online web server evaluates the general biological potency of organic drug-like molecules. This web server simultaneously predicts various types of biological activity based on the structure of organic compounds. Thus, PASS Online can be used to estimate the biological activity profile of a compound prior to its chemical synthesis and biological testing. Determination of the bioactivity of a compound based on the value of the probability "to be active" (Pa). The value of Pa ("to be active") estimates the probability that the compound studied belongs to a sub-class of active compounds based on similarity in molecular structure, which is most typical in the "active" sub-set in the PASS training set [37]. Based on the bioactivity prediction results, it shows that myricitrin has bioactivity as an antiviral (especially for influenza) with the third highest Pa value of 0.705 (Table 4) after paritaprevir (Pa value of 0.874) and remdesivir (Pa value of 0.814).

3.9. Molecular Dynamic Simulation

Molecular dynamics simulations were examined based on the root mean square deviation (RMSD), root mean square fluctuation (RMSF), and radius gyration values as a function of time. Structural variations were calculated by RMSD values of the protein-ligand complexes from 0 to 30 ns. The RMSD value continued to increase from 0 to 10 ns and reached a steady state during the simulation (Figure 10A). The average RMSD values of myricitrin were found to be 2Å. RMSD values of endoRNAse (RMSD C-alpha, RMSD Backbond, and RMSD all atoms) tend to be stable during the simulation (Figure 10B). RMSF provides the fluctuations of each atom throughout the simulation. RMSF was calculated for an endoRNAse with 346 amino acids and a potential drug candidate, myricitrin. The values confirmed that the binding site residues fluctuated less (Figure 10C). As can be seen, the ligand stabilizes the structure of the endoRNAse and its trend according to the geometric parameters (RMSF and RMSD). Those geometric parameters also indicate that myricitrin interacts stably at the binding site of endoRNAse.

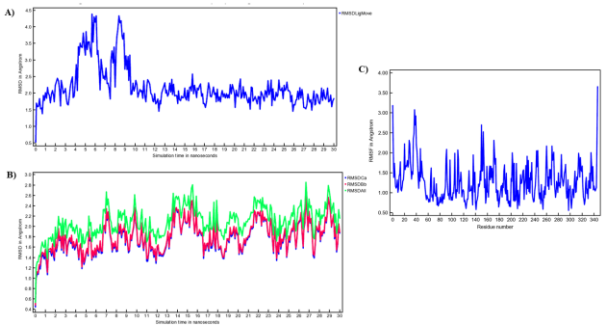

Figure 10. The plots of root mean square deviation (RMSD) ligand and protein, root mean square fluctuation (RMSF) values during 30 ns MD simulation of endoRNAse SARS-CoV-2 in complex with myricitrin

4. Conclusion

In this study, the myricitrin compound isolated and identified from E. polyanta was analyzed for its potential as a candidate for a SARS-CoV-2 antiviral drug. Analysis of the potential of myricitrin was carried out through molecular docking to a number of SARS-CoV-2 proteins (receptor binding domain on Spike/RBD, main protease/nsp5, endoRNAse, RNA-dependent-RNA-polymerase/RdRp); and its receptors, ACE2. Based on ΔG_{bind} and Ki values, myricitrin can strongly bind to the active sites on three SARS-CoV-2 proteins: endoRNAse, main protease, and RdRp. The ΔG_{bind} of myricitrin is more negative than the comparative ligands for each protein. These three proteins are potential targets for the treatment of COVID-19. Among the three proteins, myricitrin has the strongest binding affinity for endoRNAse. Myricitrin is bound stably to the active site of EndoRNAse through molecular dynamic simulations.

Acknowledgment

The authors are grateful to the Deputy for Strengthening Research and Development, Ministry of Research and Technology of the Republic of Indonesia-Research and Innovation Agency (Kemenristek-BRIN), who has financed this research under the 2020 Research Implementation Assignment Agreement Number: 1 / E1 / KP. PTNBH / 2020, dated 18 March 2020, and the Research Contract Amendment TA. 2020 Number: 1 / AMD / E1.KP.PTNBH / 2020, dated 11 May 2020.

References

[1] WHO Coronavirus (COVID-19) Dashboard, in, https://covid19.who.int/

[2] Vivi Setiawaty, Herman Kosasih, Yan Mardian, Emita Ajis, Endang Burni Prasetyowati, Siswanto, Muhammad Karyana, The identification of first COVID-19 cluster in Indonesia, *The American Journal of Tropical Medicine and Hygiene*, 103, 6, (2020), 2339-2342 https://doi.org/10.4269/ajtmh.20-0554

[3] Dewi Nur Aisyah, Chyntia Aryanti Mayadewi, Haniena Diva, Zisis Kozlakidis, Siswanto, Wiku Adisasmito, A spatial-temporal description of the SARS-CoV-2 infections in Indonesia during the first six months of outbreak, *PloS ONE*, 15, 12, (2020), e0243703 https://doi.org/10.1371/journal.pone.0243703

[4] Felipe Moura A. da Silva, Katia Pacheco A. da Silva, Luiz Paulo M. de Oliveira, Emmanoel V. Costa, Hector H. F. Koolen, Maria Lúcia B. Pinheiro, Antonia Queiroz L. de Souza, Afonso Duarte L. de Souza, Flavonoid glycosides and their putative human metabolites as potential inhibitors of the SARS-CoV-2 main protease (Mpro) and RNA-dependent RNA polymerase (RdRp), *Memórias do Instituto Oswaldo Cruz*, 115, (2020), e200207 https://doi.org/10.1590/0074-02760200207

[5] Raden Arthur Ario Lelono, Sanro Tachibana, Kazutaka Itoh, *In vitro* antioxidative activities and polyphenol content of *Eugenia polyantha* Wight grown in Indonesia, *Pakistan Journal of Biological Sciences*, 12, 24, (2009), 1564-1570 https://doi.org/10.3923/pjbs.2009.1564.1570

[6] Eisuke Kato, Ryo Nakagomi, Maria D. P. T. Gunawan-Puteri, Jun Kawabata, Identification of hydroxychavicol and its dimers, the lipase inhibitors contained in the Indonesian spice, *Eugenia polyantha*, *Food Chemistry*, 136, 3-4, (2013), 1239-1242 https://doi.org/10.1016/j.foodchem.2012.09.013

[7] R. A. A. Lelono, S. Tachibana, K. Itoh, Isolation of antifungal compounds from *Gardenia jasminoides*, *Pakistan Journal of Biological Sciences*, 12, 13, (2009), 949-956 https://doi.org/10.3923/pjbs.2009.949.956

[8] Elmar Krieger, Gert Vriend, New ways to boost molecular dynamics simulations, *Journal of Computational Chemistry*, 36, 13, (2015), 996-1007 https://doi.org/10.1002/jcc.23899

[9] Jrhau Lung, Yu - Shih Lin, Yao - Hsu Yang, Yu - Lun Chou, Li - Hsin Shu, Yu - Ching Cheng, Hung Te Liu, Ching - Yuan Wu, The potential chemical structure of anti - SARS - CoV - 2 RNA - dependent RNA polymerase, *Journal of Medical Virology*, 92, 6, (2020), 693-697 https://doi.org/10.1002/jmv.25761

[10] Christopher A. Lipinski, Lead- and drug-like compounds: the rule-of-five revolution, *Drug Discovery Today: Technologies*, 1, 4, (2004), 337-341 https://doi.org/10.1016/j.ddtec.2004.11.007

[11] Irini Doytchinova, Mariyana Atanasova, Iva Valkova, Georgi Stavrakov, Irena Philipova, Zvetanka Zhivkova, Dimitrina Zheleva-Dimitrova, Spiro Konstantinov, Ivan Dimitrov, Novel hits for acetylcholinesterase inhibition derived by docking-based screening on ZINC database, *Journal of Enzyme Inhibition and Medicinal Chemistry*, 33, 1, (2018), 768-776 https://doi.org/10.1080/14756366.2018.1458031

[12] Ajay N. Jain, Anthony Nicholls, Recommendations for evaluation of computational methods, *Journal of Computer-Aided Molecular Design*, 22, (2008), 133-139 https://doi.org/10.1007/s10822-008-9196-5

[13] Yudibeth Sixto - López, Marlet Martínez - Archundia, Drug repositioning to target NSP15 protein on SARS - CoV - 2 as possible COVID - 19 treatment, *Journal of Computational Chemistry*, 42, 13, (2021), 897-907 https://doi.org/10.1002/jcc.26512

[14] In-Wook Hwang, Shin-Kyo Chung, Isolation and identification of myricitrin, an antioxidant flavonoid, from daebong persimmon peel, *Preventive Nutrition and Food Science*, 23, 4, (2018), 341-346 https://doi.org/10.3746/pnf.2018.23.4.341

[15] Zhenming Jin, Xiaoyu Du, Yechun Xu, Yongqiang Deng, Meiqin Liu, Yao Zhao, Bing Zhang, Xiaofeng Li, Leike Zhang, Chao Peng, Yinkai Duan, Jing Yu, Lin Wang, Kailin Yang, Fengjiang Liu, Rendi Jiang, Xinglou Yang, Tian You, Xiaoce Liu, Xiuna Yang, Fang Bai, Hong Liu, Xiang Liu, Luke W. Guddat, Wenqing Xu, Gengfu Xiao, Chengfeng Qin, Zhengli Shi, Hualiang Jiang, Zihe Rao, Haitao Yang, Structure of M^{pro} from SARS-CoV-2 and discovery of its inhibitors, *Nature*, 582, (2020), 289-293 https://doi.org/10.1038/s41586-020-2223-y

[16] Youngchang Kim, Robert Jedrzejczak, Natalia I. Maltseva, Mateusz Wilamowski, Michael Endres, Adam Godzik, Karolina Michalska, Andrzej Joachimiak, Crystal structure of Nsp15 endoribonuclease NendoU from SARS - CoV - 2, *Protein Science*, 29, 7, (2020), 1596-1605 https://doi.org/10.1002/pro.3873

[17] Yushun Wan, Jian Shang, Rachel Graham, Ralph S. Baric, Fang Li, Receptor recognition by the novel coronavirus from Wuhan: an analysis based on decade-long structural studies of SARS coronavirus, *Journal of Virology*, 94, 7, (2020), https://doi.org/10.1128/jvi.00127-20

[18] Nicola E. Clarke, Martin J. Fisher, Karen E. Porter, Daniel W. Lambert, Anthony J. Turner, Angiotensin converting enzyme (ACE) and ACE2 bind integrins and ACE2 regulates integrin signalling, *PloS ONE*, 7, 4, (2012), e34747 https://doi.org/10.1371/journal.pone.0034747

[19] Xiuyuan Ou, Yan Liu, Xiaobo Lei, Pei Li, Dan Mi, Lili Ren, Li Guo, Ruixuan Guo, Ting Chen, Jiaxin Hu, Zichun Xiang, Zhixia Mu, Xing Chen, Jieyong Chen, Keping Hu, Qi Jin, Jianwei Wang, Zhaohui Qian, Characterization of spike glycoprotein of SARS-CoV-2 on virus entry and its immune cross-reactivity with SARS-CoV, *Nature Communications*, 11, (2020), 1620 https://doi.org/10.1038/s41467-020-15562-9

[20] Fang Li, Wenhui Li, Michael Farzan, Stephen C. Harrison, Structure of SARS coronavirus spike receptor-binding domain complexed with receptor, *Science*, 309, 5742, (2005), 1864-1868 https://doi.org/10.1126/science.1116480

[21] Iqrar Ahmad, Rahul Pawara, Sanjay Surana, Harun Patel, The repurposed ACE2 inhibitors: SARS-CoV-2 entry blockers of Covid-19, *Topics in Current Chemistry*, 379, (2021), 40 https://doi.org/10.1007/s41061-021-00353-7

[22] Ting Xiao, Mengqi Cui, Caijuan Zheng, Ming Wang, Ronghao Sun, Dandi Gao, Jiali Bao, Shanfa Ren, Bo Yang, Jianping Lin, Xiaoping Li, Dongmei Li, Cheng Yang, Honggang Zhou, Myricetin inhibits SARS-CoV-2 viral replication by targeting M^{pro} and ameliorates pulmonary inflammation, *Frontiers in Pharmacology*, 12, (2021), 669642 https://doi.org/10.3389/fphar.2021.669642

[23] Joshua Adedeji Bolarin, Mercy Adaramodu Oluwatoyosi, Joshua Iseoluwa Orege, Emmanuel Ayodeji Ayeni, Yusuf Ajibola Ibrahim, Sherif Babatunde Adeyemi, Bashir Bolaji Tiamiyu, Lanre Anthony Gbadegesin, Toluwanimi Oluwadara Akinyemi, Chuks Kenneth Odoh, Happiness Ijeoma Umeobi, Adenike Bernice-Eloise Adeoye, Therapeutic drugs for SARS-CoV-2 treatment: Current state and perspective, *International Immunopharmacology*, 90, (2021), 107228 https://doi.org/10.1016/j.intimp.2020.107228

[24] Natalia Fintelman-Rodrigues, Carolina Q. Sacramento, Carlyle Ribeiro Lima, Franklin Souza da Silva, Andre C. Ferreira, Mayara Mattos, Caroline S. de Freitas, Vinicius Cardoso Soares, Suelen da Silva Gomes Dias, Jairo R. Temerozo, Milene Miranda, R. Aline Matos, Fernando A. Bozza, Nicolas Carels, Carlos Roberto Alves, Marilda M. Siqueira, Patricia T. Bozza, Thiago Moreno L. Souza, Atazanavir inhibits SARS-CoV-2 replication and pro-inflammatory cytokine production (preprint), *bioRxiv*, (2020), https://doi.org/10.1101/2020.04.04.020925

[25] Otávio Augusto Chaves, Carolina Q. Sacramento, André C. Ferreira, Mayara Mattos, Natalia Fintelman-Rodrigues, Jairo R. Temerozo, Leonardo Vazquez, Douglas Pereira Pinto, Gabriel P. E. da Silveira, Laís Bastos da Fonseca, Heliana Martins Pereira, Aluana Santana Carlos, Joana C. d'Avila, João P. B. Viola, Robson Q. Monteiro, Patricia T. Bozza, Hugo Caire Castro-Faria-Neto, Thiago Moreno L. Souza, Atazanavir is a competitive inhibitor of SARS-CoV-2 M^{pro}, impairing variants replication in

vitro and in vivo, *Pharmaceuticals*, 15, 1, (2021), 21 https://doi.org/10.3390/ph15010021

[26] Xiaoyu Xue, Hongwei Yu, Haitao Yang, Fei Xue, Zhixin Wu, Wei Shen, Jun Li, Zhe Zhou, Yi Ding, Qi Zhao, Xuejun C. Zhang, Ming Liao, Mark Bartlam, Zihe Rao, Structures of two coronavirus main proteases: implications for substrate binding and antiviral drug design, *Journal of virology*, 82, 5, (2008), 2515-2527 https://doi.org/10.1128/jvi.02114-07

[27] Usman Bacha, Jennifer Barrila, Adrian Velazquez-Campoy, Stephanie A. Leavitt, Ernesto Freire, Identification of novel inhibitors of the SARS coronavirus main protease 3CL^{pro}, *Biochemistry*, 43, 17, (2004), 4906-4912 https://doi.org/10.1021/bi0361766

[28] Yan Gao, Liming Yan, Yucen Huang, Fengjiang Liu, Yao Zhao, Lin Cao, Tao Wang, Qianqian Sun, Zhenhua Ming, Lianqi Zhang, Ji Ge, Litao Zheng, Ying Zhang, Haofeng Wang, Yan Zhu, Chen Zhu, Tianyu Hu, Tian Hua, Bing Zhang, Xiuna Yang, Jun Li, Haitao Yang, Zhijie Liu, Luke W. Guddat, Quan Wang, Zhiyong Lou, Zihe Rao, Structure of the RNA-dependent RNA polymerase from COVID-19 virus, *Science*, 368, 6492, (2020), 779-782 https://doi.org/10.1126/science.abb7498

[29] Abdo A. Elfiky, SARS-CoV-2 RNA dependent RNA polymerase (RdRp) targeting: An *in silico* perspective, *Journal of Biomolecular Structure and Dynamics*, 39, 9, (2021), 3204-3212 https://doi.org/10.1080/07391102.2020.1761882

[30] Xiaominting Song, Lu Tan, Miao Wang, Chaoxiang Ren, Chuanjie Guo, Bo Yang, Yali Ren, Zhixing Cao, Yuzhi Li, Jin Pei, Myricetin: A review of the most recent research, *Biomedicine & Pharmacotherapy*, 134, (2021), 111017 https://doi.org/10.1016/j.biopha.2020.111017

[31] Susan A. Olender, Katherine K. Perez, Alan S. Go, Bindu Balani, Eboni G. Price-Haywood, Nirav S. Shah, Su Wang, Theresa L. Walunas, Shobha Swaminathan, Jihad Slim, BumSik Chin, Stéphane De Wit, Shamim M. Ali, Alex Soriano Viladomiu, Philip Robinson, Robert L. Gottlieb, Tak Yin Owen Tsang, I-Heng Lee, Hao Hu, Richard H. Haubrich, Anand P. Chokkalingam, Lanjia Lin, Lijie Zhong, B. Nebiyou Bekele, Robertino Mera-Giler, Chloé Phulpin, Holly Edgar, Joel Gallant, Helena Diaz-Cuervo, Lindsey E. Smith, Anu O. Osinusi, Diana M. Brainard, Jose I. Bernardino, Remdesivir for severe coronavirus disease 2019 (COVID-19) versus a cohort receiving standard of care, *Clinical Infectious Diseases*, 73, 11, (2021), e4166-e4174 https://doi.org/10.1093/cid/ciaa1041

[32] Ashleigh Shannon, Nhung Thi-Tuyet Le, Barbara Selisko, Cecilia Eydoux, Karine Alvarez, Jean-Claude Guillemot, Etienne Decroly, Olve Peersen, Francois Ferron, Bruno Canard, Remdesivir and SARS-CoV-2: Structural requirements at both nsp12 RdRp and nsp14 Exonuclease active-sites, *Antiviral Research*, 178, (2020), 104793 https://doi.org/10.1016/j.antiviral.2020.104793

[33] Toshie Manabe, Dan Kambayashi, Hiroyasu Akatsu, Koichiro Kudo, Favipiravir for the treatment of patients with COVID-19: a systematic review and meta-analysis, *BMC Infectious Diseases*, 21, (2021), 489 https://doi.org/10.1186/s12879-021-06164-x

[34] Inge Hamming, Wim Timens, M. L. C. Bulthuis, A. T. Lely, G. J. van Navis, Harry van Goor, Tissue distribution of ACE2 protein, the functional receptor for SARS coronavirus. A first step in understanding SARS pathogenesis, *The Journal of Pathology: A Journal of the Pathological Society of Great Britain and Ireland*, 203, 2, (2004), 631-637 https://doi.org/10.1002/path.1570

[35] Muchtaridi Muchtaridi, M. Fauzi, Nur Kusaira Khairul Ikram, Amirah Mohd Gazzali, Habibah A. Wahab, Natural flavonoids as potential angiotensin-converting enzyme 2 inhibitors for anti-SARS-CoV-2, *Molecules*, 25, 17, (2020), 3980 https://doi.org/10.3390/molecules25173980

[36] P. S. Kulkarni, Y. S. Walunj, N. D. Dongare, Theoretical Validation of Medicinal Properties of *Ocimum sanctum*, *The Chemist*, 92, 1, (2021), 1-7

[37] S. Parasuraman, Prediction of activity spectra for substances, *Journal of Pharmacology & Pharmacotherapeutics*, 2, 1, (2011), 52-53 https://doi.org/10.4103/0976-500X.77119